

Research

Open Access

## Tissue Doppler imaging of carotid plaque wall motion: a pilot study

Kumar V Ramnarine\*<sup>1</sup>, Tim Hartshorne<sup>2</sup>, Yvonne Sensier<sup>2</sup>, May Naylor<sup>2</sup>, Joanne Walker<sup>2</sup>, A Ross Naylor<sup>2</sup>, Ronney B Panerai<sup>1</sup> and David H Evans<sup>1</sup>

Address: <sup>1</sup>Department of Medical Physics, University Hospitals of Leicester NHS Trust, Leicester, UK and <sup>2</sup>Department of Surgery, University Hospitals of Leicester NHS Trust, Leicester, UK

Email: Kumar V Ramnarine\* - kumar.ramnarine@uhl-tr.nhs.uk; Tim Hartshorne - tim.hartshorne@uhl-tr.nhs.uk; Yvonne Sensier - yvonne-sensier@uhl-tr.nhs.uk; May Naylor - may.naylor@uhl-tr.nhs.uk; Joanne Walker - joanne.walker@uhl-tr.nhs.uk; A Ross Naylor - ross.Naylor@uhl-tr.nhs.uk; Ronney B Panerai - rp9@leicester.ac.uk; David H Evans - dhe@leicester.ac.uk

\* Corresponding author

Published: 19 December 2003

Received: 17 November 2003

*Cardiovascular Ultrasound* 2003, 1:17

Accepted: 19 December 2003

This article is available from: <http://www.cardiovascularultrasound.com/content/1/1/17>

© 2003 Ramnarine et al; licensee BioMed Central Ltd. This is an Open Access article: verbatim copying and redistribution of this article are permitted in all media for any purpose, provided this notice is preserved along with the article's original URL.

### Abstract

**Background:** Studies suggest the physical and mechanical properties of vessel walls and plaque may be of clinical value in the diagnosis and treatment of cardiovascular atherosclerotic disease. The purpose of this pilot study was to investigate the potential clinical application of ultrasound Tissue Doppler Imaging (TDI) of Arterial Wall Motion (AWM) and to quantify simple wall motion indices in normal and diseased carotid arteries.

**Methods:** 224 normal and diseased carotid arteries (0–100% stenoses) were imaged in 126 patients (age 25–88 years, mean  $68 \pm 11$ ). Longitudinal sections of the carotid bifurcation were imaged using a Philips HDI5000 scanner and L12-5 probe under optimized TDI settings. Temporal and spatial AWMs were analyzed to evaluate the vessel wall displacements and spatial gradients at peak systole averaged over 5 cardiac cycles.

**Results:** AWM data were successfully extracted in 91% of cases. Within the carotid bifurcation/plaque region, the maximum wall dilation at peak systole ranged from -100 to 750 microns, mean  $335 \pm 138$  microns. Maximum wall dilation spatial gradients ranged 0–0.49, mean  $0.14 \pm 0.08$ . The AWM parameters showed a wide variation and had poor correlation with stenoses severity. Case studies illustrated a variety of pertinent qualitative and quantitative wall motion features related to the biophysics of arterial disease.

**Conclusion:** Our clinical experience, using a challenging but realistic imaging protocol, suggests the use of simple quantitative AWM measures may have limitations due to high variability. Despite this, pertinent features of AWM in normal and diseased arteries demonstrate the potential clinical benefit of the biomechanical information provided by TDI.

### Background

Cardiovascular disease accounts for around half the deaths in the Western world, with stroke being the third leading cause of death and disability worldwide [1]. The predictive ability to identify which patients will have a stroke is poor. Current clinical practice for selecting which

patients will have a carotid endarterectomy, to reduce the risk of stroke, relies on assessment of the degree of arterial lumen narrowing. Large European [2] and North American [3] clinical trials have demonstrated the benefit of carotid endarterectomy on groups of patients with severe stenosis. However the degree of stenosis is a poor

predictor of individual stroke risk, and treatment of asymptomatic patients remains controversial [4]. Recent studies on improved predictors of stroke risk have focused on the assessment of plaque morphology, composition, and the mechanical properties of the vessel wall and plaque deposit [5-12].

Researchers have long hoped that the physical and mechanical properties of arteries may be of clinical value in the diagnosis and treatment of cardiovascular disease [13,14]. The carotid artery is a useful window for cardiovascular risk, with ultrasound able to provide unique information on morphological, hemodynamic and elastic properties [14]. Numerous studies have shown that the elastic properties of arteries may be useful in the study of cardiovascular disease. The localized mechanical properties of carotid plaque and the vessel wall may be of particular value in identifying plaque vulnerable to rupture. The majority of clinical wall motion studies have derived elasticity parameters from measurements of the wall motion at a single location in vessels. Vessels have included the common carotid artery [15,16], femoral artery [15], brachial artery [17,18], cerebral arteries [19] and aorta [20,21].

Various ultrasound techniques have been used to detect and track the vessel wall motion. Computational techniques have mainly been based on analysis of the B-mode greyscale images [18,22,23], M-mode [16], analyses of the raw RF ultrasound data [24] and Doppler techniques [20,25]. Tissue Doppler Imaging (TDI) is a relatively new commercial technique, originally developed for imaging the myocardium, which has found increasing applications in echocardiography. TDI is basically a colour Doppler technique that has been optimised to provide images of tissue motion rather than blood flow, and is capable of high spatial and temporal resolution. The signal processing techniques employed to extract the tissue velocity information from the RF ultrasound data are typically based on time domain cross-correlation techniques [26] or autocorrelation techniques [27]. Clinical applications of TDI of the myocardium, including theoretical, pathophysiological and methodological considerations are reviewed elsewhere [28]. TDI has been applied to image arterial wall motion patterns of the common carotid artery (CCA) and to assess CCA stiffness by calculating distensibility as the change in normalised mean systolic distension relative to the change in blood pressure, and compliance as the change in cross-sectional area relative to pulse pressure [29].

Atherosclerotic plaque typically develops around the region of the internal and common carotid artery bifurcation. Knowledge of the differential wall motion displacements across the carotid bifurcation in normal and in

diseased arteries may thus be useful in the study of atherosclerotic disease. An important clinical application is the identification of high-risk plaques that are vulnerable to rupture, leading to stroke. It is hoped the vulnerable plaque may be predicted by identifying pertinent features of the carotid plaque wall motion behaviour throughout the cardiac cycle. Initial clinical studies, using a TDI technique that was optimised to study carotid arterial wall motion (AWM) highlighted a number of case examples of carotid plaque disease suggesting the potential clinical use of AWM imaging [30].

The purpose of this study was to investigate the possible clinical value of these recent TDI techniques for AWM imaging in the vascular examination. In particular, this study assessed the dynamic wall motion deformation behavior of the carotid plaque and vessel wall. Arterial wall motion indices were quantified in a wide spectrum of normal and diseased carotid arteries to quantify baseline parameters, assess variability and help assess future clinical potential.

## Methods

### Subjects

224 carotid arteries were scanned in 126 patients and volunteers (age 25–88 years, mean  $68 \pm 11$ ) with a wide spectrum of carotid disease. Patients presenting through the Leicester Royal Infirmary vascular studies unit for carotid artery studies were recruited. Thus, the majority of patients presented with medical conditions including cardiovascular disease (over 90% of subjects) and hypertension (blood pressure greater than 140 mmHg systole or 90 mmHg diastole in approximately 65% of subjects, as measured following ultrasound scan, using an Omron 705CP monitor and cuff over the brachial artery). The 4 volunteers were young and healthy, with no history of cardiovascular disease and no ultrasound evidence of atherosclerotic disease. 70 subjects were male and 56 were female with mean systolic and diastolic blood pressures of  $152 \pm 24$  mmHg and  $83 \pm 13$  mmHg (mean  $\pm 1$  standard deviation) respectively. In accordance with the Helsinki declaration, informed consent and Ethical approval for the study was obtained. In total, 58 carotid arteries were imaged from patients with no ultrasound evidence of atherosclerotic disease, and 166 arteries imaged with ultrasound evidence of atherosclerotic disease.

### Ultrasound equipment

This study used an Arterial Wall Motion (AWM) imaging facility developed by Philips Research Laboratories using novel Tissue Doppler Imaging signal processing techniques [26]. The AWM software was able to assess, along a 3–4 cm length, the arterial wall velocities and displacements, and to derive vessel compliance, tissue elasticity and stress/strain images. This additional information on

the biomechanical nature of the artery and plaque deposit is available throughout the cardiac cycle.

An ATL HDI5000 ultrasound scanner and an L12-5 linear array probe (Philips Medical Systems, Andover, US) with Tissue Doppler Imaging (TDI) mode was used to scan a longitudinal section of the vessel. Ultrasound scanning was performed by experienced vascular sonographers. Ultrasound data was collected from diseased carotid arteries at the location of stenotic plaque at the bifurcation of the common carotid artery (CCA) and the proximal internal carotid artery (ICA). In patients with no ultrasound evidence of stenoses, data was collected from the common carotid bifurcation including longitudinal segments of the ICA and the CCA. TDI data was collected over 6 cardiac cycles using optimal and standardized machine settings as follows: image depth adjusted to display the carotid image in longitudinal view; 2D Opt Parameter set to Pen.; Color and TDI imaging set to ON; Tissue Opt Parameter set to Gen.; Colour Line Density set to A; colour sensitivity set to Medium; colour smoothing set to Off; colour DMD set to Off; colour Persistence set to Off; no beam steering of TDI colour box; Velocity scale set to 1.4 cm/sec to avoid aliasing of wall motion data and maintain high frame rate; colour gain set to 100%.

#### **Data analysis**

The ultrasound data were stored as cineloop digital data files. Data were analyzed off-line using Philips Research Link HDILAB analysis software and the Arterial Wall Motion proprietary software developed by Philips Research Laboratories [26,30]. The software provided values for the axial wall dilations (defined as the difference between the anterior and posterior wall diameters relative to the reference diastole values) along a longitudinal segment of the artery for each image frame. Scan line spatial resolution was 0.148 mm, temporal resolution between 30–45 Hz and wall displacement resolution of a few microns. These data were exported to MATLAB™ (The MathWorks, Inc., Natick, MA, US) for data analysis. The wall displacements at peak systole were averaged over 5 cardiac cycles. The data were then divided into 3 segments corresponding to the ICA segment, the plaque region (or the carotid bulb in normal arteries) and the CCA segment. The location of the vessel boundaries were based on the ultrasound images. An additional quantitative criteria was used to precisely define the boundary based on the first derivative (gradient) of the spatial wall dilation having a value of 0. In each of the 3 regions, the maximum and minimum wall displacements were quantified and also the maximum and minimum spatial gradients along the longitudinal artery segments. Statistical analysis was performed using the unpaired Student's t-Test to determine if there is a significant difference between the means of two sample populations ( $p < 0.05$ ).

## **Results**

### **Case examples of arterial wall motion in normal carotid arteries**

Figure 1 shows an example of synchronized, spatially homogeneous arterial wall motion of the common carotid artery proximal to the carotid bifurcation of a normal vessel with no ultrasound evidence of atherosclerotic disease. Figure 2 shows an example of synchronized, spatially homogeneous arterial wall motion at the carotid bifurcation of a normal vessel with no ultrasound evidence of atherosclerotic disease. See Additional file 1: AVI movie file of Figure 2. Figure 3 shows an example of inhomogeneous arterial wall motion at the carotid bifurcation of a normal vessel with no ultrasound evidence of atherosclerotic disease. See Additional file 2: AVI movie file of Figure 3.

### **Case examples of arterial wall motion in diseased carotid arteries**

Figure 4 shows an example of arterial wall motion across a plaque with a mild 30% stenosis (diameter reduction). See Additional file 3: AVI movie file of Figure 4. Figure 5 shows an example of arterial wall motion across a plaque with 70% stenosis (diameter reduction). High dilation gradients at the plaque vessel interface and localized stiffening with constricted wall motion at the plaque are demonstrated. See Additional file 4: AVI movie file of Figure 5. Figure 6 shows an example of arterial wall motion across a plaque with a severe 80% stenosis (diameter reduction). See Additional file 5: AVI movie file of Figure 6. Figure 7 shows an interesting example of an ulcerated plaque and highlights the uncertainty over the wall tracking across the lumen in these tuning fork bifurcations when the ICA and external carotid artery (ECA) are in the same plane. The lower ICA has been selected for wall tracking by the user selecting a point within the lumen of the ICA. At the bifurcation, the wall tracking has a discontinuity across the lumen of the ECA. The example highlights the requirement for careful interpretation of the AWM data. Figure 8 shows an example of a severe stenosis in which the vessel wall is poorly defined and the reliability of the AWM tracking algorithm is uncertain.

### **Quantification of simple AWM indices**

Figures 9 and 10 show the respective quantification results for the minimum and maximum wall dilations, and the wall dilation spatial gradients in each of the 3 arterial segments. Maximum and minimum wall dilations at peak systole were plotted as a function of stenosis severity. The significant difference between the maximum and minimum values of the wall dilation within the plaque highlights the inhomogeneous wall motion within the plaque, but it is also due to the criteria used to identify the vessel boundaries. The greater wall motion inhomogeneity in the plaque region is also indicated by the significantly

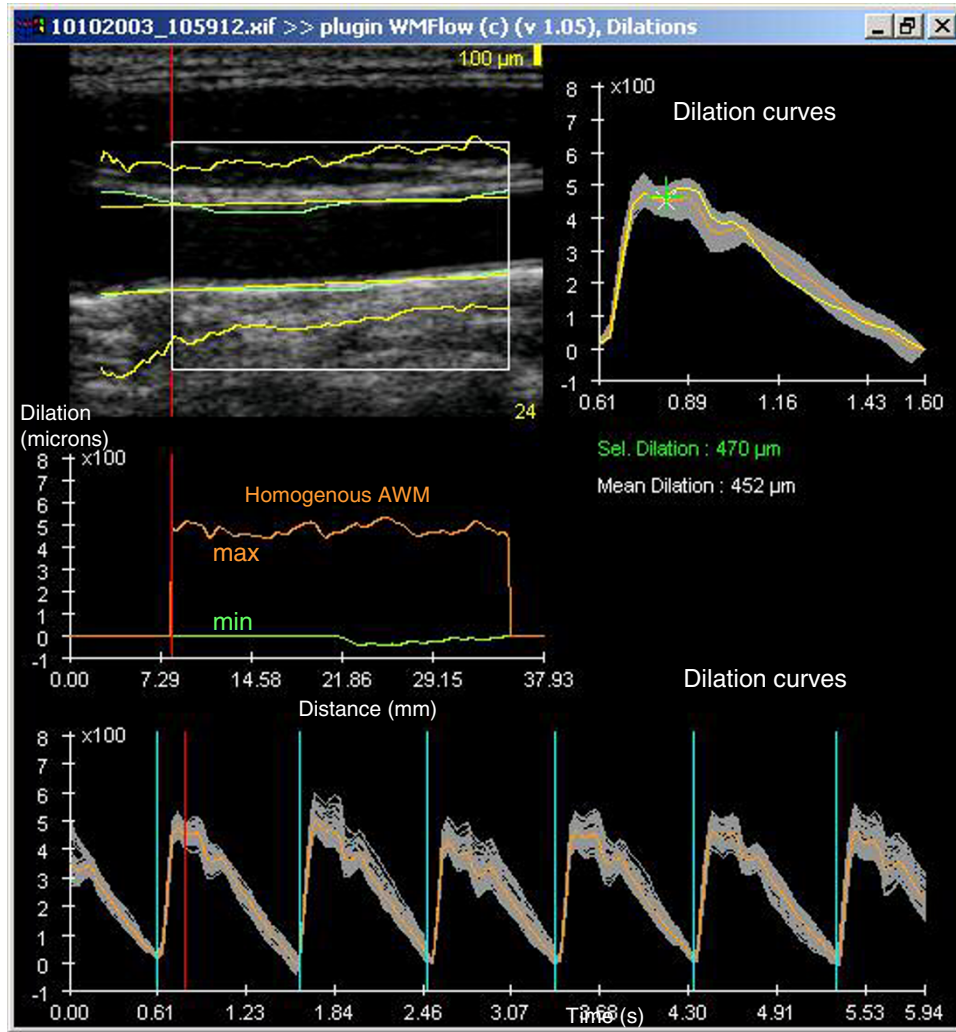


**Figure 1**

**homogeneous arterial wall motion of a normal CCA segment.** The region of interest (ROI) is positioned over a straight longitudinal section of the CCA proximal to the carotid bulb. The wall displacements along the artery are superimposed on a magnified graphic scale relative to the initial baseline dilation reference positions (yellow lines). The green lines map the vessel walls of each image frame, based on an edge detection algorithm using the 2D image information. The middle image shows the maximum (orange line) and minimum (green line) displacements within the cardiac cycle selected by the red vertical line in the bottom image. The bottom image shows the spatial wall displacements as a function of time, showing the dilation curves for each scan line (approximately 200 lines, separated by 0.148 mm). The blue vertical lines indicate the start of each cardiac cycle. The orange dilation curves correspond to the mean wall displacements in the ROI. The top right figure shows the wall displacements for the selected cardiac cycle, highlighting in yellow the wall displacements at the location selected by the vertical red line in the ultrasound image.



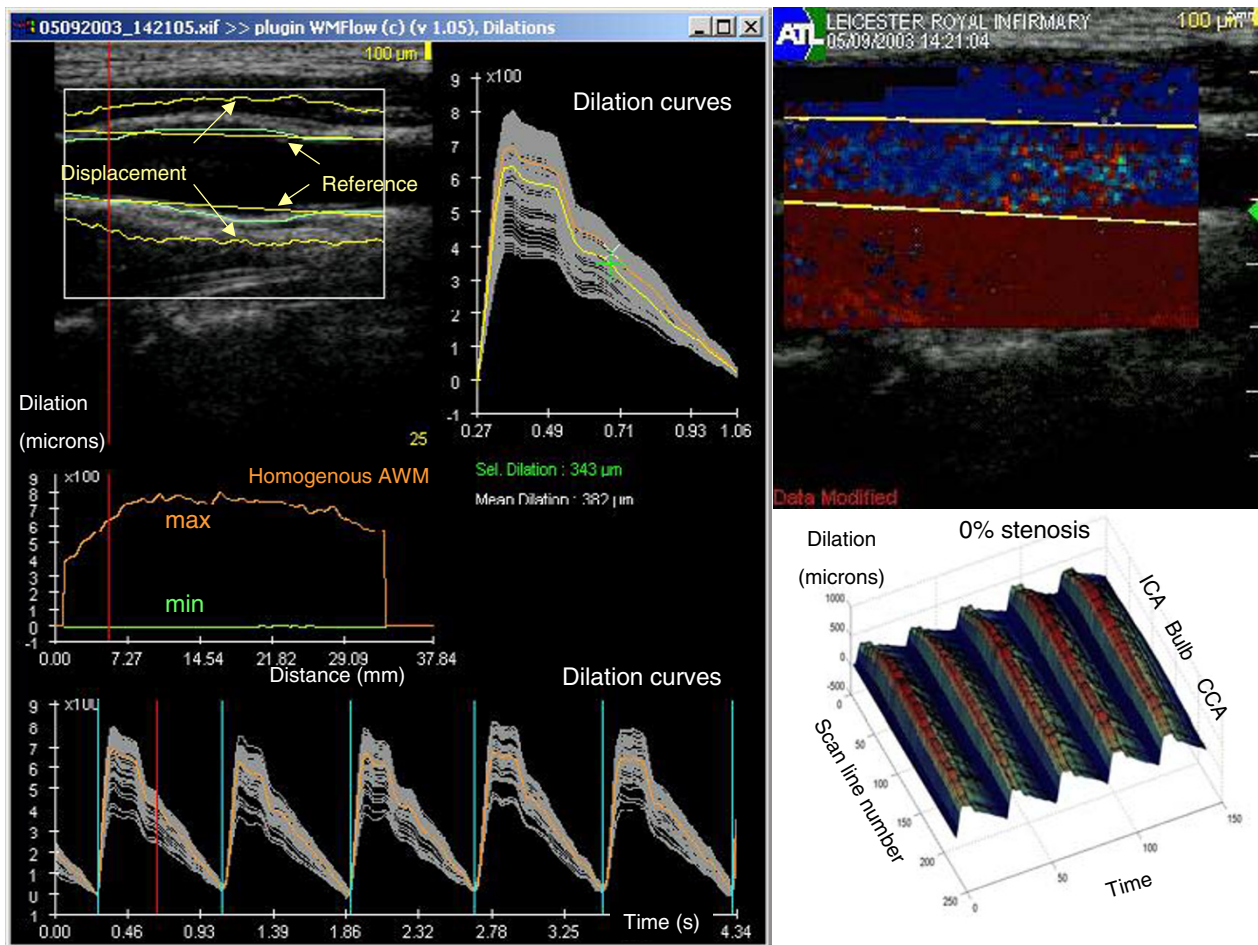


**Figure 2**  
**homogeneous arterial wall motion at the carotid bifurcation of normal arteries.** This shows an example of synchronized, spatially homogeneous arterial wall motion at the carotid bifurcation of a normal artery with no ultrasound evidence of atherosclerotic disease. See Additional file 1 for the real-time movie of the top right image. The lower right graph displays the dilation data as a surf plot with dilation plotted as a function of the spatial position and the time.

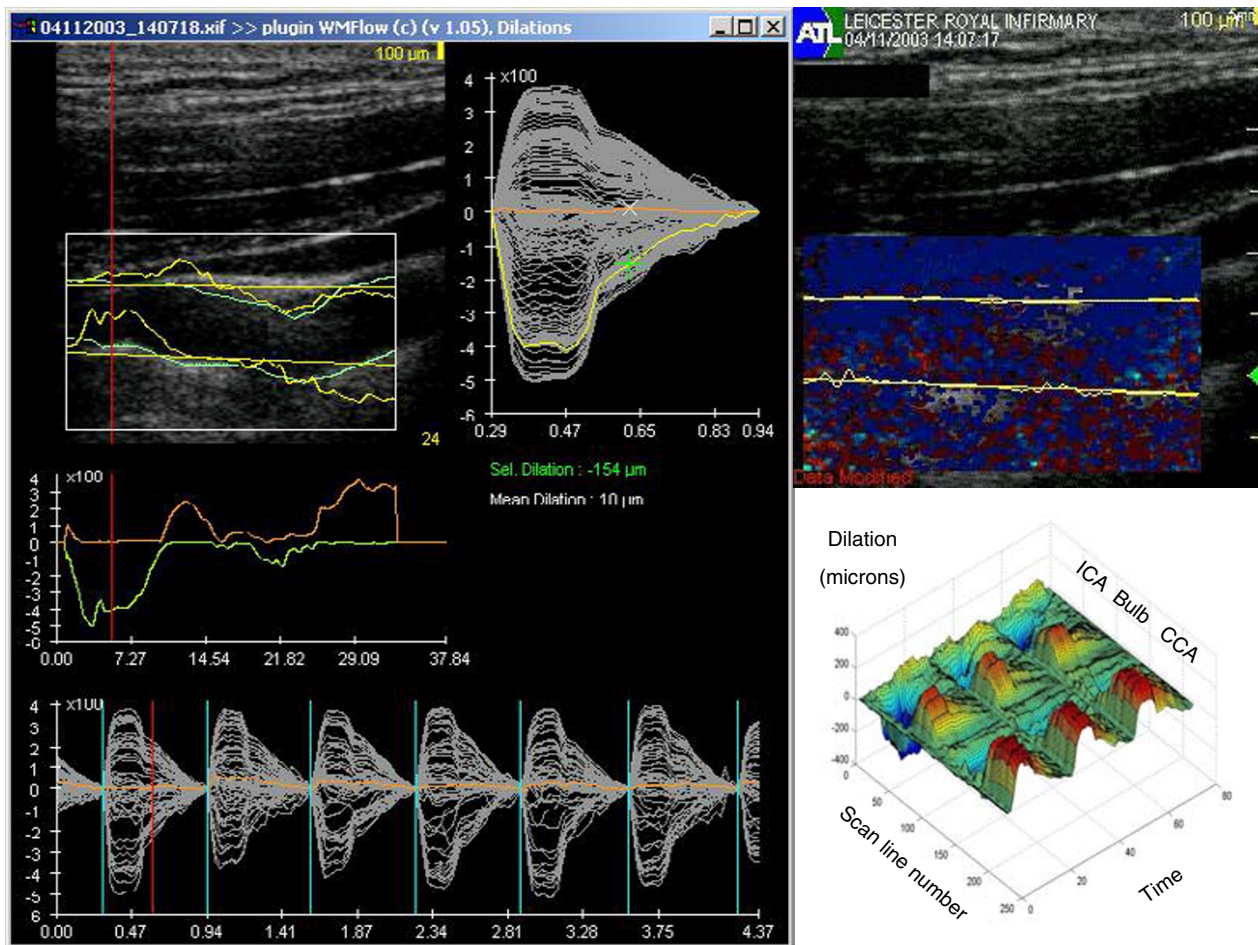
higher spatial gradient values ( $p < 0.0001$ ) compared with the ICA and the CCA. The variability of the wall motion indices are wide with no significant dependence on plaque severity (% stenosis). Even in arteries with no plaque, the 0% stenoses cases, the wall dilation measures vary widely. The segments of the ICA and the CCA also display wide variability in the wall motion indices.

Table 1 summarises the AWM dilation measures within segments of the ICA, the plaque (carotid bulb) and the CCA. Table 2 summarises the arterial wall motion spatial gradients within segments of the ICA, the plaque (carotid bulb) and the CCA.

**Discussion**

This is the first study to assess the clinical feasibility of TDI of carotid plaque wall motion using subjective and quantitative measures in a wide spectrum of normal and diseased arteries. Currently, clinically useful endpoints are based on morphological and hemodynamic properties of arteries. Extension of the ultrasound vascular examination to provide clinically useful vascular endpoints associated with the mechanical behaviour of carotid plaque may also be useful for characterising plaque.

Wall motion behaviour within a straight segment of the CCA typically displays synchronized, spatially homogeneous wall motion (Figure 1). This type of homogeneous wall motion is typically observed in normal straight



**Figure 3**  
**Inhomogeneous arterial wall motion at the carotid bifurcation of normal torturous arteries.** This shows an example of inhomogeneous arterial wall motion at the carotid bifurcation of normal arteries with no ultrasound evidence of atherosclerotic disease. Note torturous artery with significant compression within the ICA due to posterior wall displacement. See Additional file 2 for the real-time movie of the top right image. The lower right graph displays the dilation data as a surf plot with dilation plotted as a function of the spatial position and the time.

segments of individual vessels and is in accord with previous studies on the normal CCA [31]. An important potential application of measuring carotid plaque wall motion is to help identify the unstable plaque at high risk of rupture and consequent stroke. As plaque typically develops in the region of the carotid bifurcation, this study used a challenging imaging protocol that included the plaque (carotid bulb in normal arteries), the proximal segment of the ICA and the CCA. A variety of wall motion features were observed in a wide spectrum of normal and diseased arteries. The wall motion across the carotid bifurcation, even in vessels with no plaque may exhibit more complex behaviour than single vessels segments. Figure 2 shows an example of homogeneous wall motion across the bifurcation in a normal subject with no atherosclerotic disease.

This is in contrast to more complex wall motion across the bifurcation (Figure 3) observed in a different subject, also with no evidence of atherosclerotic disease. This differential wall motion across the carotid bifurcation is not uncommon and represents a confounding factor in the use of our simple quantification measures for the differentiation of normal and diseased vessels. The variability may reflect true differences in wall motion between the different regions (ICA, carotid bulb and CCA). However, it is also likely, at least in part, to be caused by limitations and artefacts from various potential sources that we discuss later.

The dynamic wall motion deformation behaviour appears to provide potentially useful information on the elastic



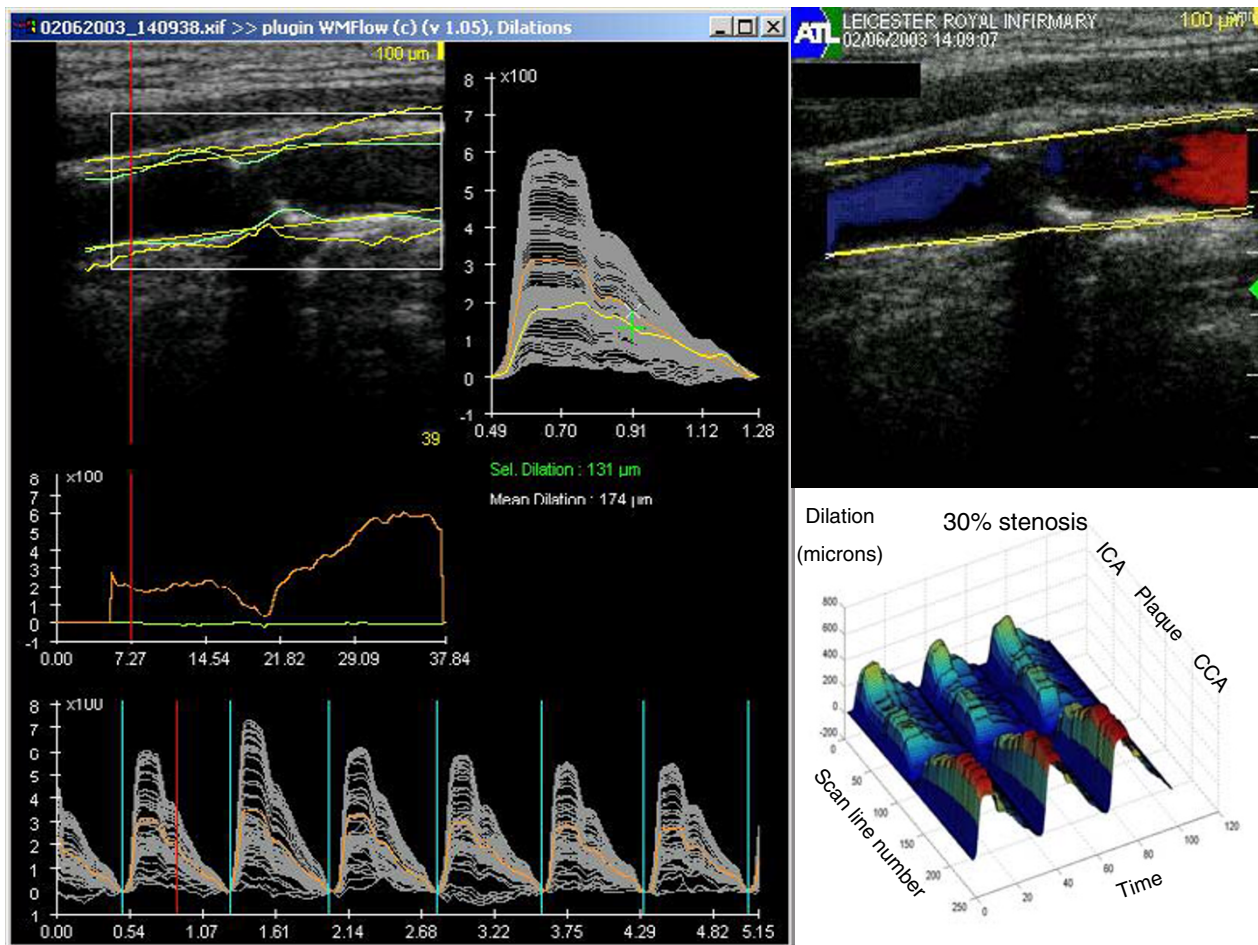


**Figure 4**  
**Local arterial wall motion stiffening around a mild stenosis calcified plaque.** This shows an example of arterial wall motion across a calcified plaque with a mild 30% stenosis (diameter reduction). Note the localised stiffening and high dilation gradients. See Additional file 3 for the real-time movie of the top right image. The lower right graph displays the dilation data as a surf plot with dilation plotted as a function of the spatial position and the time.

nature of the vessels walls. A variety of common features were observed in patients with a wide range of atherosclerotic plaque disease. The clinical case studies illustrated in Figures 4, 5, 6 demonstrate a variety of pertinent qualitative and quantitative wall motion features related to the biophysics of arterial disease. These included examples of AWM constriction or stiffening associated with calcified plaque, constriction due to pressure drop through a severe stenosis (Venturi effect), high spatial gradient and intraplaque/vessel-interface inhomogeneities which were related to plaque type and severity. Pertinent features associated with clinical end points such as plaque development, plaque rupture and stroke are important and will require additional follow up studies.

It is also important to appreciate the potential problems and reliability of the technique. The clinical case examples in Figures 3, 7 and 8 showed examples of variable AWM behavior that did not appear to relate to plaque disease. These highlighted potential limitations of the technique and the use of simple quantification indices. Our simple AWM indices, which included the minimum and maximum wall dilations and spatial wall dilation gradients, showed a wide variation and generally had poor correlation with stenosis severity. The sources of error and variability may arise from various sources including the equipment, the operator, the patient and the limitations and design of our pilot study. A brief summary of some important considerations is given below.

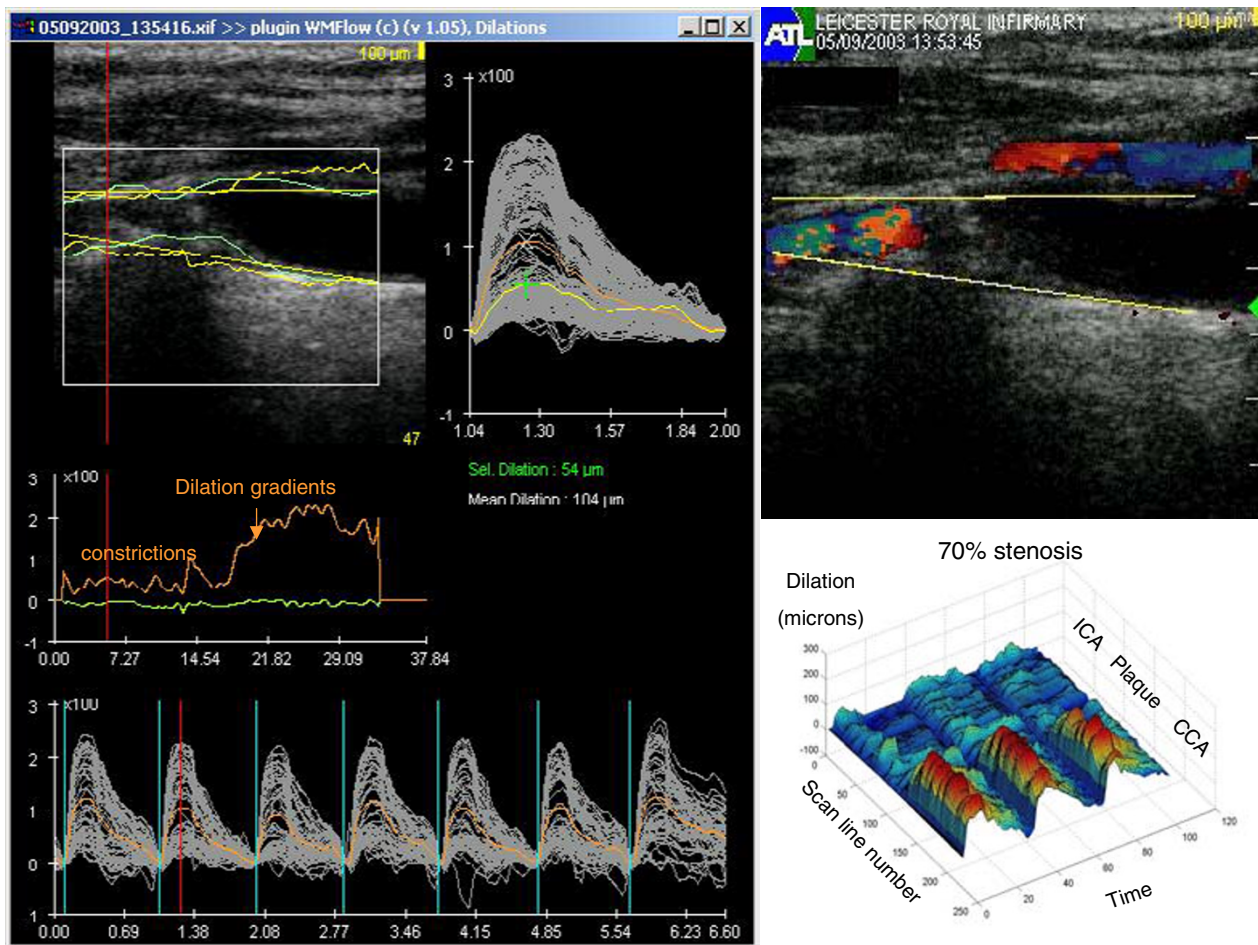


**Figure 5**  
**Arterial wall motion stiffening around a severe stenosis plaque.** Figure 5 shows an example of arterial wall motion across a plaque with 70% stenosis (diameter reduction). High dilation gradients at the plaque vessel interface and localized stiffening with constricted wall motion at the plaque are demonstrated. See Additional file 4 for the real-time movie of the top right image. The lower right graph displays the dilation data as a surf plot with dilation plotted as a function of the spatial position and the time.

**Limitations and sources of error**

*Equipment*

The AWM system was fundamentally limited to the measurement of wall motion within the beam scan plane and in the direction of the ultrasound pulse. TDI velocity data is angle dependent and provides the velocity component in scan plane only. The transverse component (perpendicular to the beam) of carotid plaque wall motion is also significant and may be of potential clinical importance. Indeed this transverse motion of the artery, synchronized with the arterial blood flow, is often apparent from the grayscale and color Doppler images.

The TDI AWM signal processing algorithm is based on a cross correlation technique on multiple RF signals. The

characteristics, performance and limitations of the algorithm from a signal processing perspective are discussed elsewhere [26,32]. The performance of the TDI technique has been evaluated using *in-vitro* test phantoms developed to assess the performance for measurements of the tissue motion of the myocardium [33]. Studies have also used *in-vitro* phantoms and flow models to assess accuracy, variability and reproducibility of the TDI AWM technique [34]. One study [34], using a commercial polyurethane flow phantom, showed the intrinsic spatial and temporal stability was 2.46% with accuracy of 5.36%. However, the applicability of these *in-vitro* measurements in providing a realistic assessment of the *in-vivo* clinical measurements is likely to depend on the characteristics and properties of the test phantoms. We have shown that use of agar based



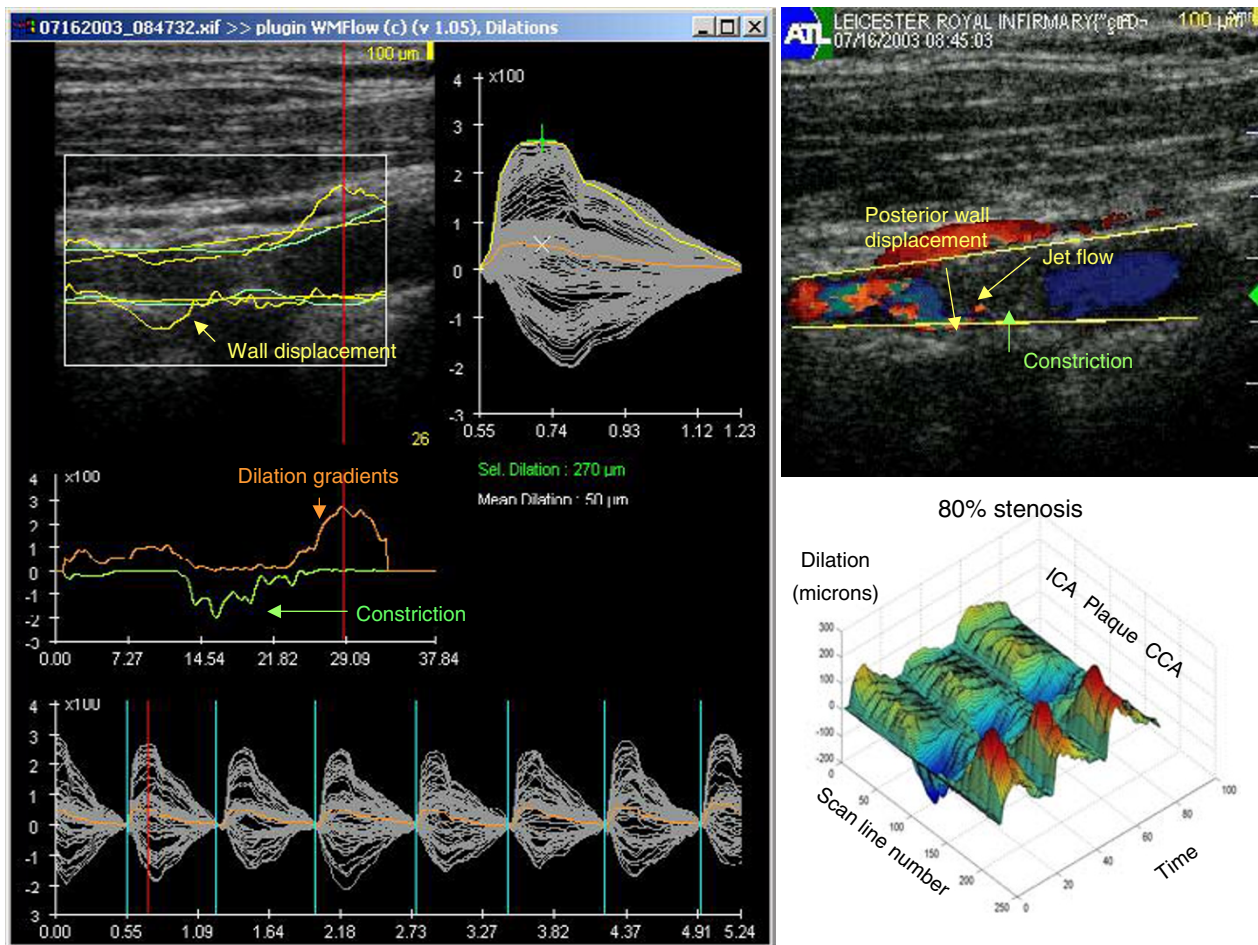


**Figure 6**  
**Complex arterial wall motion across a plaque with a severe 80% stenosis.** This shows an example of arterial wall motion across a plaque with a severe 80% stenosis (diameter reduction). The high velocity jet flow hits against the posterior wall which shows marked wall displacements distal to the plaque. Within the plaque there is significant vessel wall constriction due to the pressure drop within the lumen. This is an example of the Venturi effect, well known in fluid dynamics in which the increased kinetic energy of blood flow through the constriction corresponds to a pressure drop and consequent constriction of the vessel walls. See Additional file 5 for the real-time movie of the top right image. The lower right graph displays the dilation data as a surf plot with dilation plotted as a function of the spatial position and the time.

tissue mimicking wall-less flow phantoms [35], with Rayleigh scattering characteristics are likely to provide a more challenging assessment of wall motion compared to phantoms with well defined specular wall /interface reflections [36].

**Operator**

Variations in wall motion quantification may arise due to inter- and intra- operator variability. Experienced ultrasonographers are required to optimise wall tracking performance. Positioning of the transducer to maintain good vessel wall definition across the carotid bifurcation whilst avoiding excessive transducer pressure and potential arte-

facts from the neighbouring jugular vein are important considerations.

Important factors include the orientation of the scan plane and beam vessel angle, optimization of image quality, operator steadiness, transducer contact pressure and selection of machine settings (settings were standardized in this study).

**Patient**

For the clinical application of identifying the vulnerable plaque, or characterizing plaque type, confounding factors and sources of variability may arise from the patient.

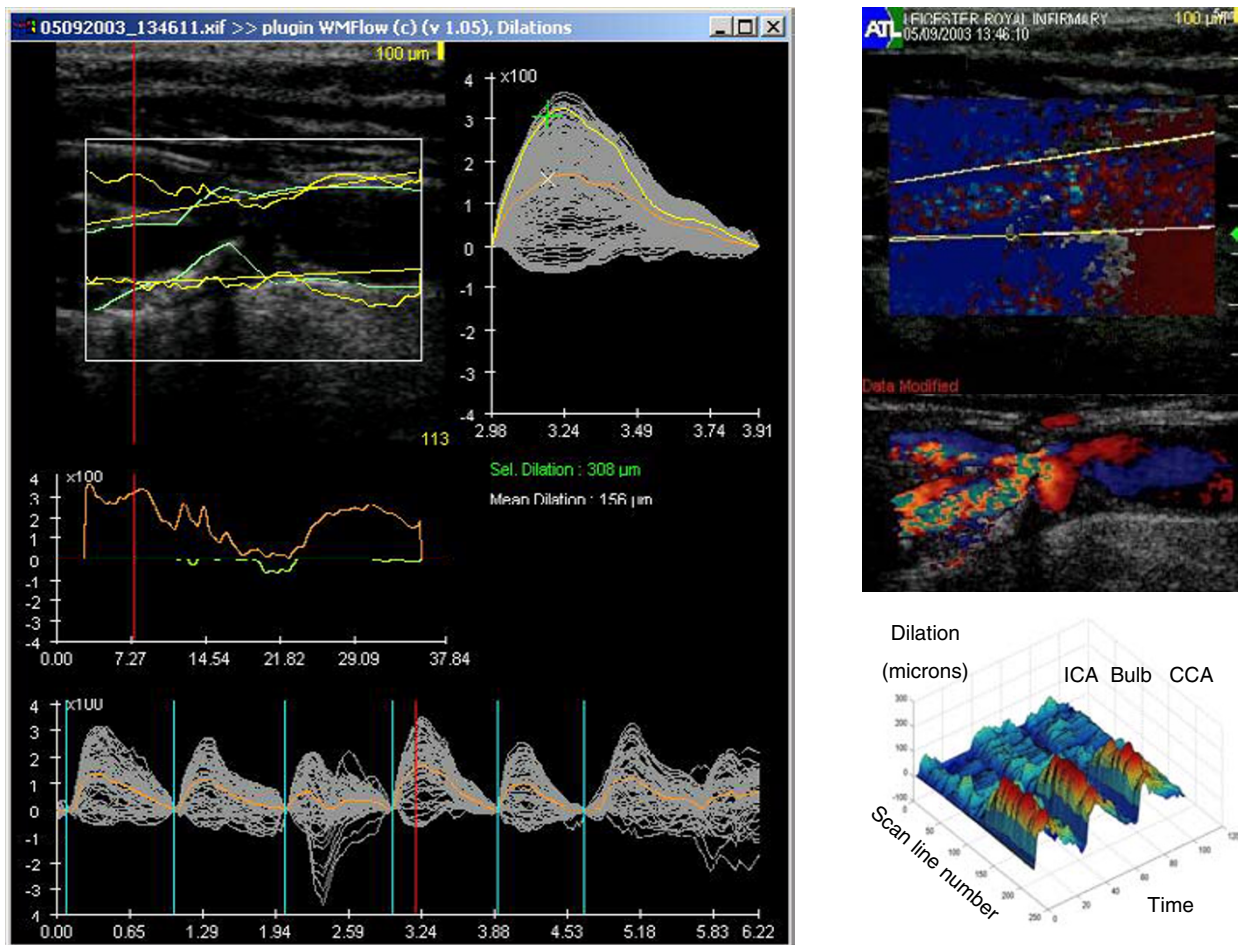


**Figure 7**  
**Limitations of arterial wall motion tracking across the vessel lumen.** This shows an interesting example of an ulcerated plaque and highlights the uncertainty over the wall tracking across the lumen in these tuning fork bifurcations. At the bifurcation, the wall tracking of the ICA has a discontinuity across the lumen of the ECA. The example highlights the requirement for careful interpretation of the AWM data.

**Table 1: Arterial wall motion dilation within segments of the CCA, plaque deposit (bifurcation in normal arteries) and the ICA.**

Location	Mean (microns)	SD (microns)	Minimum (microns)	Maximum (microns)
CCA				
Min wall dilation	253	128	-93	712
Max wall dilation	334	132	41	750
Plaque (bifurcation)				
Min wall dilation	4	130	-526	593
Max wall dilation	335	138	-100	750
ICA				
Min wall dilation	42	100	-273	386
Max wall dilation	167	127	-110	706

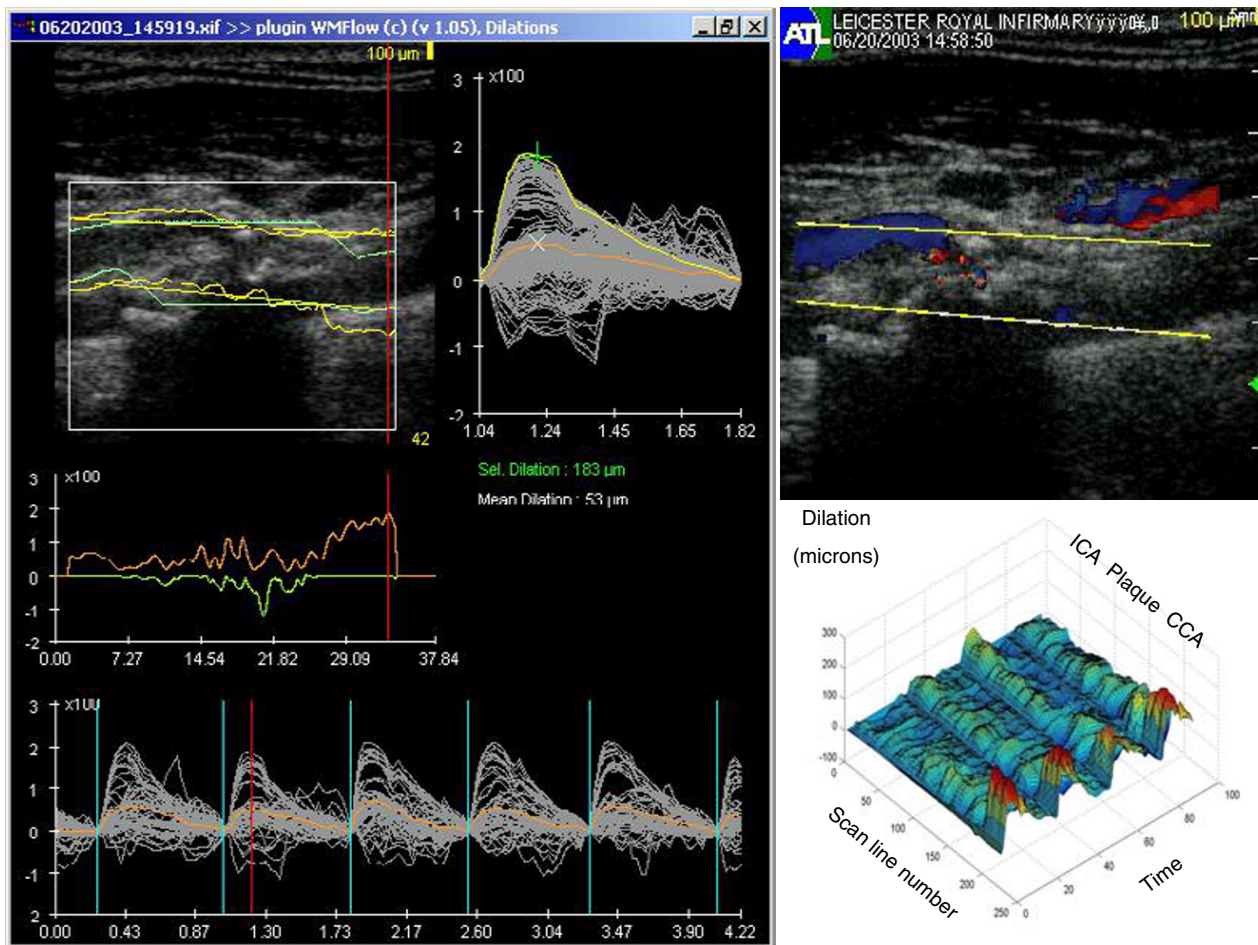


**Figure 8**  
**Limitations of arterial wall motion tracking in severe disease.** This shows an example of a severe stenosis in which the vessel wall is poorly defined and the reliability of the AWM tracking is uncertain.

**Table 2: Arterial wall motion spatial gradients within segments of the CCA, plaque deposit (carotid bulb in normal arteries) and the ICA.**

Location	Mean	SD	Min	Max
CCA spatial gradient	0.073	0.057	0	0.47
Plaque (bulb) spatial gradient	0.14	0.079	0	0.49
ICA spatial gradient	0.11	0.073	0	0.42

Wall motion and the elastic properties of arteries have been shown to be related to the patient's age, sex, pathology and physiology [37,38]. Variations in anatomy, and breathing/motion artifacts are also likely to increase the variability of wall motion quantification measures. Geometrical deviations of the vessels from the perpendicular and variation of image quality and vessel wall definition

will have a deleterious effect on the wall tracking algorithm.

*Pilot Study*

Our pilot study of clinical potential used a challenging but realistic imaging protocol that encompassed the carotid bifurcation. In contrast to measurements on a single



## Arterial Wall Motion Quantification: Minimum and Maximum Dilation Indices

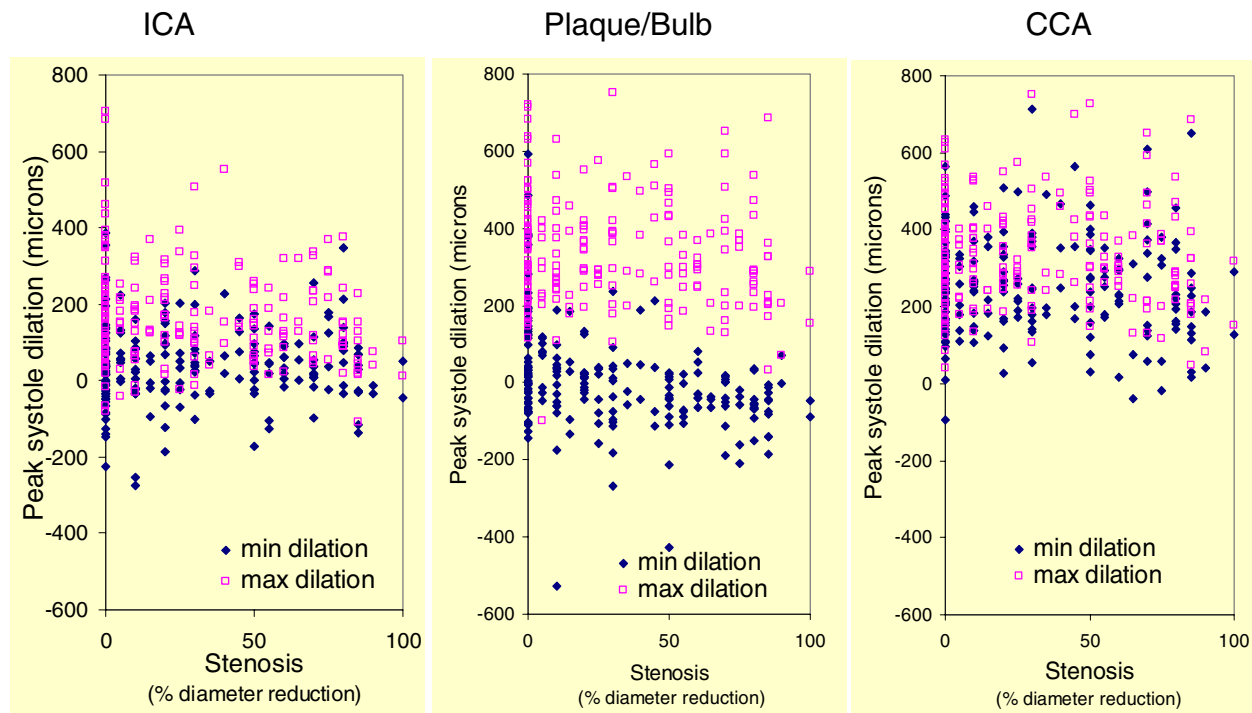


**Figure 9**  
Arterial wall dilation as a function of stenosis severity for segments of the ICA, the plaque (carotid bulb) and the CCA.

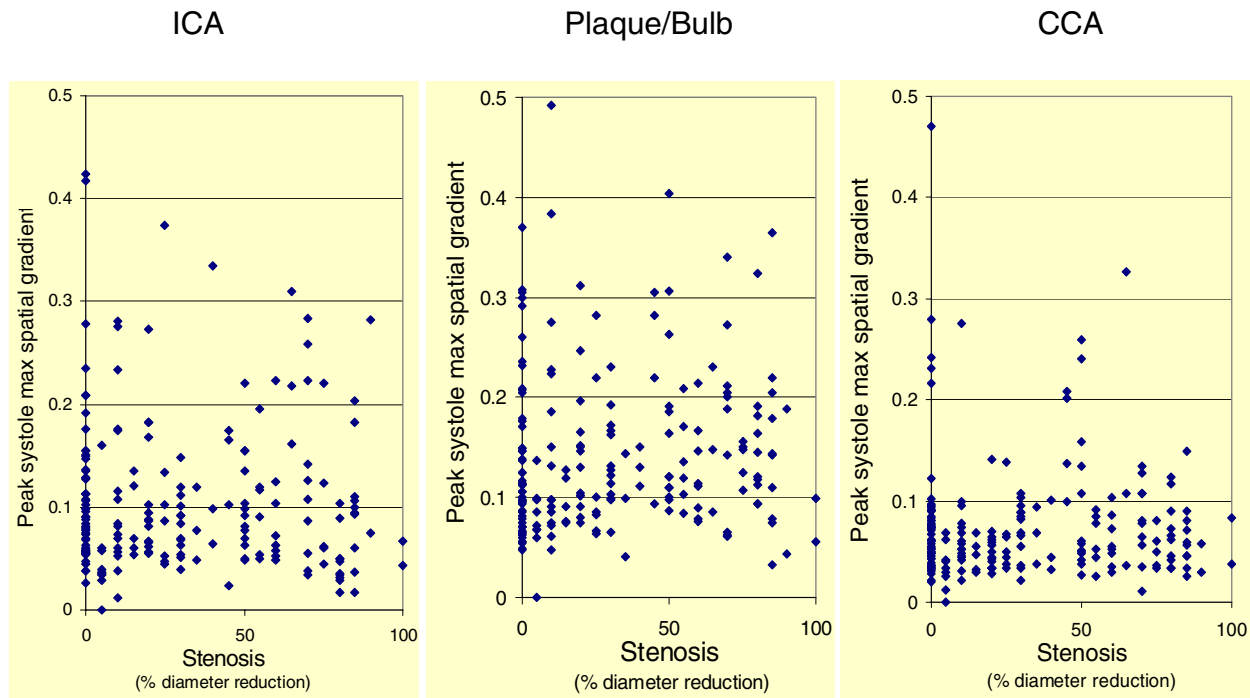
straight artery segment, there are greater variations in the size, shape, angle and image quality across the bifurcation. Inherent local variations may also exist in the mechanical behavior and properties of the different segments. However, this is the clinically realistic site of interest for the clinical application of identifying the vulnerable plaque.

Only the simplest of wall motion measures, the dilations and spatial gradients at peak systole were quantified. Additional parameters and more sophisticated characterization of the dynamic wall motion patterns in normal and diseased arteries may provide a more suitable and clinically useful vascular measure. Other measures, for spatial and temporal wall motion homogeneity have been described [31].

The design of our pilot study accentuated the variability as no attempt was made to discard cases due to technical or other artifacts. Only 9% of cases were discarded prior to quantification. These were due to difficulties with data collection at the carotid bifurcation or failure of the AWM software to discriminate between consecutive cardiac cycle wall motion. In order to avoid potential bias by subjective discrimination, all AWM results were pooled, including outliers with apparent artifacts. This approach also helped assess the potential for routine application of the TDI technique as an extension to the vascular examination. A further subjective assessment of the scans could reject cases that suffer from poor image quality, wall tracking problems, anatomical variations etc.

There was no gold standard for plaque characterization and the type of plaque in case examples were based on the ultrasound grayscale appearance. Further work and fol-

## Arterial Wall Motion Quantification: Maximum Spatial Dilatation Gradient Indices

**Figure 10**

Arterial wall dilation spatial gradients as a function of stenosis severity for segments of the ICA, the plaque (carotid bulb) and the CCA.

low-up studies are required to assess interesting characteristics of the plaque (area, homogeneity, histology, composition, mechanical and physical properties) as well as the carotid vessels (intima-media thickness, kinking, stenosis in series, stenosis of contralateral carotid bifurcation). Finally, there is no gold standard to compare the *in-vivo* equipment performance, as the spatial and temporal resolution performance capabilities are unique to the ultrasound TDI technique.

### Conclusions

Our pilot study demonstrates that the TDI Arterial Wall Motion imaging technique provides an impressive biomechanical window to atherosclerotic disease. It provides potentially useful information on the dynamic behavior of normal and diseased carotid arteries. Our initial clinical experience, using a challenging but realistic protocol for imaging carotid plaque wall motion, suggests the use of simple quantitative AWM measures may have limitations

due to high variability. The technique must be robust and shown to be clinically useful if it is to play a major role in the vascular examination, where it is hoped that assessment of the mechanical properties of arteries, may help to provide a more rational basis for referring patients to carotid surgery.

### Competing interests

None declared.

### Authors' contributions

KVR conceived of the study, participated in its design and coordination, analyzed the data and drafted the manuscript.

TH, YS, MN and JW recruited patients, collected and reviewed the ultrasound data.

ARN recruited patients.

RBP and DHE participated in the study design and coordination.

All authors read, commented and approved the final manuscript.

## Additional material

### Additional File 1

Example of synchronized, spatially homogeneous arterial wall motion at the carotid bifurcation of a normal vessel with no ultrasound evidence of atherosclerotic disease.

Click here for file  
[<http://www.biomedcentral.com/content/supplementary/1476-7120-1-17-S1.avi>]

### Additional File 2

Example of inhomogeneous arterial wall motion at the carotid bifurcation of a normal vessel with no ultrasound evidence of atherosclerotic disease. Note torturous artery with significant compression within the ICA due to posterior wall displacement.

Click here for file  
[<http://www.biomedcentral.com/content/supplementary/1476-7120-1-17-S2.avi>]

### Additional File 3

Example of arterial wall across a calcified plaque with a mild 30% stenosis (diameter reduction). Note the localised stiffening and high dilation gradients.

Click here for file  
[<http://www.biomedcentral.com/content/supplementary/1476-7120-1-17-S3.avi>]

### Additional File 4

Example of arterial wall motion across a plaque with 70% stenosis (diameter reduction). High dilation gradients at the plaque vessel interface and localized stiffening with constricted wall motion at the plaque are demonstrated.

Click here for file  
[<http://www.biomedcentral.com/content/supplementary/1476-7120-1-17-S4.avi>]

### Additional File 5

Example of arterial wall motion across a plaque with a severe 80% stenosis (diameter reduction). The high velocity jet flow hits against the posterior wall which shows marked wall displacements proximal to the plaque. Within the plaque there is significant vessel wall constriction due to the pressure drop within the lumen. This is an example of the Venturi effect, well known in fluid dynamics in which the increased kinetic energy of blood flow through the constriction corresponds to a pressure drop and consequent constriction of the vessel walls. See Additional file 5 for the real-time movie of the top right image. The lower right graph displays the dilation data as a surf plot with dilation plotted as a function of the spatial position and the time.

Click here for file  
[<http://www.biomedcentral.com/content/supplementary/1476-7120-1-17-S5.avi>]

## Acknowledgements

This work was funded by a Research Award of University Hospitals of Leicester NHS Trust. The authors are grateful for the support of Mr Terry Hayes of Philips Medical Systems.

## References

- Murray CJ, Lopez AD: **Mortality by cause for eight regions of the world: Global Burden of Disease Study.** *Lancet* 1997, **349(9061)**:1269-76.
- European Carotid Surgery Trial Collaborators: **Randomised trial of endarterectomy for recently symptomatic carotid stenosis: final results of the MRC European Carotid Surgery Trial (ECST).** *Lancet* 1998, **351(9113)**:1379-87.
- North American Symptomatic Carotid Endarterectomy Trial Collaborators: **Beneficial effect of carotid endarterectomy in symptomatic patients with high-grade carotid stenosis.** *N Engl J Med* 1991, **325(7)**:445-53.
- Barnett HJ, Meldrum HE, Eliasziw M, North American Symptomatic Carotid Endarterectomy Trial (NASCET) collaborators: **The appropriate use of carotid endarterectomy.** *CMAJ* 2002, **166(9)**:1169-79.
- Bang J, Dahl T, Bruinsma A, Kaspersen JH, Nagelhus Hernes TA, Myhre HO: **A new method for analysis of motion of carotid plaques from RF ultrasound images.** *Ultrasound Med Biol* 2003, **29(7)**:967-76.
- Bank AJ, Versluis A, Dodge SM, Douglas WH: **Atherosclerotic plaque rupture: a fatigue process?** *Med hypotheses* 2000, **55(6)**:480-484.
- Cheng KS, Baker CR, Hamilton G, Hoeks AP, Seifalian AM: **Arterial elastic properties and cardiovascular risk/event.** *Eur J Vasc Endovasc Surg* 2002, **24(5)**:383-97.
- Golemati S, Sassano A, Lever MJ, Bharath AA, Dhanjil S, Nicolaides AN: **Carotid artery wall motion estimated from B-mode ultrasound using region tracking and block matching.** *Ultrasound Med Biol* 2003, **29**:387-99.
- Laurent S, Katsahian S, Fassot C, Tropeano AI, Gautier I, Laloux B, Boutouyrie P: **Aortic stiffness is an independent predictor of fatal stroke in essential hypertension.** *Stroke* 2003, **34(5)**:1203-1206.
- Oliver JJ, Webb DJ: **Noninvasive assessment of arterial stiffness and risk of atherosclerotic events.** *Arteriosclerosis Thromb Vasc Biol* 2003, **23**:554-566.
- Plett MI, Beach KW, Dunmire B, Brown KG, Primozich JF, Strandness E: **In vivo ultrasonic measurement of tissue vibration at a stenosis: A case study.** *Ultrasound Med Biol* 2001, **27(8)**:1049-1058.
- Richardson PD: **Biomechanics of plaque rupture: progress, problems, and new frontiers.** *Ann Biomed Eng* 2002, **30(4)**:524-36.
- Dobrin PB: **Mechanical properties of arteries.** *Physiol Rev* 1978, **58(2)**:397-460.
- Nagai Y, Matsumoto M, Metter EJ: **The carotid artery as a noninvasive window for cardiovascular risk in apparently healthy individuals.** *Ultrasound Med Biol* 2002, **28(10)**:1231-8.
- Balkestein EJ, Staessen JA, Wang JG, van Der Heijden-Spek JJ, Van Bortel LM, Barlassina C, Bianchi G, Brand E, Herrmann SM, Struijker-Boudier HA: **Carotid and femoral artery stiffness in relation to three candidate genes in a white population.** *Hypertension* 2001, **38(5)**:1190-7.
- Kanters SD, Elgersma OE, Banga JD, van Leeuwen MS, Algra A: **Reproducibility of measurements of intima-media thickness and distensibility in the common carotid artery.** *Eur J Vasc Endovasc Surg* 1998, **16(1)**:28-35.
- Kaiser DR, Mullen K, Bank AJ: **Brachial artery elastic mechanics in patients with heart failure.** *Hypertension* 2001, **38(6)**:1440-5.
- Beux F, Carmassi S, Salvetti MV, Ghiadoni L, Huang Y, Taddei S, Salvetti A: **Automatic evaluation of arterial diameter variation from vascular echographic images.** *Ultrasound Med Biol* 2001, **27(12)**:1621-9.
- Hayashi K, Handa H, Nagasawa S, Okumura A, Moritake K: **Stiffness and elastic behavior of human intracranial and extracranial arteries.** *J Biomech* 1980, **13(2)**:175-84.
- Lehmann ED: **Elastic properties of the aorta.** *Lancet* 1993, **342**:1417.

21. Sonesson B, Hansen F, Lanne T: **Abdominal aortic aneurysm: a general defect in the vasculature with focal manifestations in the abdominal aorta?** *J Vasc Surg* 1997, **26(2)**:247-54.
22. Stadler RW, Taylor JA, Lees RS: **Comparison of B-mode, M-mode and echo-tracking methods for measurement of the arterial distension waveform.** *Ultrasound Med Biol* 1997, **23(6)**:879-87.
23. Newey VR, Nassiri DK: **Online artery diameter measurement in ultrasound images using artificial neural networks.** *Ultrasound Med Biol* 2002, **28(2)**:209-16.
24. Hoeks AP, Brands PJ, Smeets FA, Reneman RS: **Assessment of the distensibility of superficial arteries.** *Ultrasound Med Biol* 1990, **16(2)**:121-8.
25. Hoeks AP, Brands PJ, Reneman RS: **Assessment of the arterial distension waveform using Doppler signal processing.** *J Hypertens Suppl* 1992, **10(6)**:S19-22.
26. Bonnefous O, Montaudon M, Sananes JC, Denis E: **Noninvasive Echographic Techniques for Arterial Wall Characterization.** *IEEE Ultrason Symp Proc* 1996:1059-1064.
27. Kasai C, Namekawa K, Koyano A, Omoto R: **Real-Time Two-Dimensional Blood Flow Imaging Using an Autocorrelation Technique.** *IEEE Trans Sonics Ultrasonics* 1985, **32**:458-463.
28. Mundigler G, Zehetgruber M: **Tissue Doppler Imaging: Myocardial velocities and strain-are there clinical applications?** *J Clin Basic Cardiol* 2002, **5**:125-132.
29. Schmidt-Trucksass A, Grathwohl D, Schmid A, Boragk R, Upmeier C, Keul J, Huonker M: **Assessment of carotid wall motion and stiffness with tissue Doppler imaging.** *Ultrasound Med Biol* 1998, **24(5)**:639-646.
30. Bonnefous O, Luisy F, Kownator S: **Arterial wall motion imaging: a new ultrasound approach to vascular characterisation.** *Medica Mundi* 2000, **44(2)**:37-43.
31. Meinders JM, Brands PJ, Willigers JM, Kornet L, Hoeks AP: **Assessment of the spatial homogeneity of artery dimension parameters with high frame rate 2D B-mode.** *Ultrasound Med Biol* 2001, **27(6)**:785-94.
32. Ferrara K, DeAngelis G: **Color flow mapping.** *Ultrasound Med Biol* 1997, **23(3)**:321-45.
33. Nowicki A, Olszewski R, Etienne J, Karłowicz P, Adamus J: **Assessment of wall velocity gradient imaging using a test phantom.** *Ultrasound Med Biol* 1996, **22(9)**:1255-60.
34. Germond I, Bonnefous O, Loupas T: **Quantitative assessment of the artery dilation measurements with an arterial phantom.** *IEEE Ultrasonics Symp* 2001:1413-1416.
35. Ramnarine KV, Anderson T, Hoskins PR: **Construction and geometric stability of physiological flow rate wall-less stenosis phantoms.** *Ultrasound Med Biol* 2001, **27(2)**:245-50.
36. Kanber B, Ramnarine KV, Panerai RB: **A probabilistic approach to computerised tracking of arterial wall motion from grayscale images [abstract].** *Br J Rad* in press.
37. Reneman RS, Hoeks APG, Westerhof N: **Non-invasive assessment of artery wall properties in humans-methods and interpretation.** *J Vasc Invest* 1996, **2(2)**:53-64.
38. Reneman RS, van Merode T, Brands PJ, Hoeks AP: **Inhomogeneities in arterial wall properties under normal and pathological conditions.** *J Hypertens Suppl* 1992, **10(6)**:S35-9.

Publish with **BioMed Central** and every scientist can read your work free of charge

"BioMed Central will be the most significant development for disseminating the results of biomedical research in our lifetime."

Sir Paul Nurse, Cancer Research UK

Your research papers will be:

- available free of charge to the entire biomedical community
- peer reviewed and published immediately upon acceptance
- cited in PubMed and archived on PubMed Central
- yours — you keep the copyright

Submit your manuscript here:  
[http://www.biomedcentral.com/info/publishing\\_adv.asp](http://www.biomedcentral.com/info/publishing_adv.asp)

